



In vitro and *in vivo* studies on the biocompatibility of a self-powered pacemaker with a flexible buckling piezoelectric vibration energy harvester for rats

Feng Xie¹, Xiaoqing Qian^{2,3}, Ning Li⁴, Daxiang Cui³, Hao Zhang⁴, Zhiyun Xu^{1,4}

¹Department of Cardiovascular Surgery, Changhai Hospital, Naval Military Medical University, Shanghai, China; ²School of Biomedical Engineering, Shanghai Jiaotong University, Shanghai, China; ³Department of Instrument Science & Engineering, School of Electronic Information & Electrical Engineering, Shanghai Engineering Research Center for Intelligent Diagnosis & Treatment Instrument, Institute of Nano Biomedicine & Engineering, Shanghai Jiaotong University, Shanghai, China; ⁴Institute of Cardiothoracic Surgery at Changhai Hospital, Second Military Medical University, Shanghai, China

Contributions: (I) Conception and design: F Xie, H Zhang; (II) Administrative support: Z Xu, D Cui; (III) Provision of study materials or patients: X Qian; (IV) Collection and assembly of data: N Li; (V) Data analysis and interpretation: F Xie; (VI) Manuscript writing: All authors; (VII) Final approval of manuscript: All authors.

Correspondence to: Daxiang Cui. Department of Instrument Science & Engineering, School of Electronic Information & Electrical Engineering, Shanghai Engineering Research Center for Intelligent Diagnosis & Treatment Instrument, Institute of Nano Biomedicine & Engineering, Shanghai Jiaotong University, 800 Dongchuan Rd., Shanghai 200240, China. Email: dx cui@sjtu.edu.cn; Hao Zhang; Zhiyun Xu. Institute of Cardiothoracic Surgery at Changhai Hospital, Second Military Medical University, Shanghai 200433, China. Email: zhanghao@smmu.edu.cn; zhiyunx@hotmail.com.

Background: Scavenging energy from biomechanical motions *in vivo* by energy converting devices, i.e., implantable harvesters, to obtain sustainable electrical energy is the ideal way to power implantable medical devices which require long term and continuous power supply. A novel self-powered cardiac pacemaker is designed to achieve self-powered pacing. The kinetic energy of the heart was collected by an implanted piezoelectric energy collector and supplied to the cardiac pacemaker, and then the cardiac tissue was stimulated by the pacing electrode pierced from the outside of the heart to realize effective pacing effect and self-powered pacing. In this study, we evaluated the stability and biocompatibility of our previously described flexible buckling piezoelectric vibration energy harvester *in vitro* and *in vivo*. The biocompatibility, *in vivo* stability, and safety of the self-powered pacemaker with a flexible flexion piezoelectric vibratory energy harvesting device prepared were analyzed by performing cell and *in vivo* animal experiments.

Methods: The MTT(3-(4,5-Dimethylthiazol-2-yl)-2,5-diphenyltetrazolium bromide) assay was used to detect the cell proliferation of H9C2 cells and HUVECs at 24, 48, and 72 hours. Computed tomography (CT) and cardiac ultrasound were used to evaluate the position and heart rate of pacemakers 12 weeks after implantation, and the changes of plasma biochemical indexes were detected by a biochemical detector.

Results: At 12 weeks after implantation, CT results showed that there were no changes in the position of the self-powered pacemaker. The device implanted into the thoracic cavity of rats demonstrated certain effects on cardiac function, while it did not have a significant effect on their blood biochemical indexes.

Conclusions: the flexible buckling piezoelectric vibratory energy collector did not produce adverse effects on the myocardial tissue or on the normal proliferation of myocardial cells.

Keywords: Piezoelectric vibration energy harvesters; cardiac pacemaker; implantable medical devices; biocompatibility; biosafety

Submitted Mar 18, 2021. Accepted for publication Apr 28, 2021.

doi: 10.21037/atm-21-1707

View this article at: <http://dx.doi.org/10.21037/atm-21-1707>

Introduction

In the last 20 years, cardiac pacemakers have achieved great advances, but the basic system of extravascular pulse generators, in contact with cardiac tissue, and the battery-based power supply methods are underdeveloped. Most of the complications associated with pacemakers, such as infection, pneumothorax, lead failure, and ineffective pacing, are related to the basic system and battery-based approaches to power supply, especially batteries and leads. In addition, to ensure adequate power sources, regular replacement of the battery has become a major problem for pacemaker patients. Thus, researchers have increasingly turned their focus towards developing wireless, self-powered pacemakers.

Cardiac pacemakers, which are one of the most common implantable medical electronic therapeutic devices for assisting cardiac function in clinic practice (1), generate an electrical pulse powered by a battery through a pulse generator (2). By using a wire electrode and stimulating the electrode exposed to the cardiac muscle, the cardiac pacemaker excites the heart to contract, thereby successfully combating energy shortage caused by cardiac dysfunction, heart failure(3). At present, millions of patients are dependent on implantable medical devices such as pacemakers to maintain normal vital signs (4). In the past half century, significant progresses have been made in the studies of pacemakers, but the Basic system of extravascular pulse generator for cardiac tissues and battery-powered method is less developed and infrastructure to support pacing (5,6). However, pacemakers are associated with many unfavorable complications. Serious potential pulmonary complications, such as pneumothorax, pneumonia, respiratory failure, and chronic obstructive pulmonary disease exacerbation, may also occur after pacemaker treatment (7-9), which are mainly caused by batteries and wires. In addition, to ensure an adequate power supply, regular replacement of the battery can greatly increase the health risks of patients. Therefore, the development of wireless and self-powered pacemakers has become the main research direction of future pacemakers.

Researchers have made great efforts in developing self-powered medical devices. The optimal approach is to directly convert biomechanical energy (e.g., muscle stretching, heartbeat, blood flow, gas flow due to respiration, etc.) into electrical energy (10,11). The mechanisms of biomechanical energy conversion include electromagnetic induction, triboelectricity, static electricity, and piezoelectric

electricity (12,13). Among them, the piezoelectric method shows great potential in implantable self-powered medical devices, due to its high-power density, high output stability, and device flexibility (14,15). However, it is still a struggle to directly power commercial pacemakers with an implantable piezoelectric energy collector. Adequate power output has become a key challenge in driving pacemakers with implantable piezoelectric energy harvester, while the efficiency of the piezoelectric energy collector is closely related to the piezoelectric materials, manufacturing process, structure design, implantation location, and piezoelectric energy harvesting mode.

Therefore, we prepared a flexible buckling piezoelectric vibration energy collector in our early study stage (2 years ago), however, the toxicity and biocompatibility of this energy collector in cells have not been studied. We conducted a 12-week stability and safety experiment of the energy collector in rats for more accurate results. Our data indicated that the flexible buckling piezoelectric vibrational energy harvester had no adverse effects on myocardial tissue or the proliferation of myocardial cells. At 12 weeks after implantation, computed tomography (CT) showed that there were no changes in the position of the self-powered pacemaker. Ultrasonography showed that rat heart rate and systolic function were normal, and there were no significant effects on the blood biochemical indexes of the rats.

We present the following article in accordance with the ARRIVE reporting checklist (available at <http://dx.doi.org/10.21037/atm-21-1707>).

Methods

Material preparation

The completed flexible buckling piezoelectric vibration energy collector was prepared (*Figure 1*). *Figure 1A* is the concept diagram of the self-powered pacemaker system. As shown in *Figure 1B*, the system is mainly composed of a piezoelectric energy collector unit, a pacing probe, a pulse generator circuit unit, and an external packaging unit. The piezoelectric energy converter provides power to a pulse-generator circuit, which produces effective electrical stimulation to cardiac tissues through a pacing probe inserted from outside the heart. The self-energy supply of the piezoelectric energy collection method and epicardial pacing are the basis of the feasibility of the device. *Figure 1C* shows the device diagram of the piezoelectric energy collector created to verify the feasibility of the device,

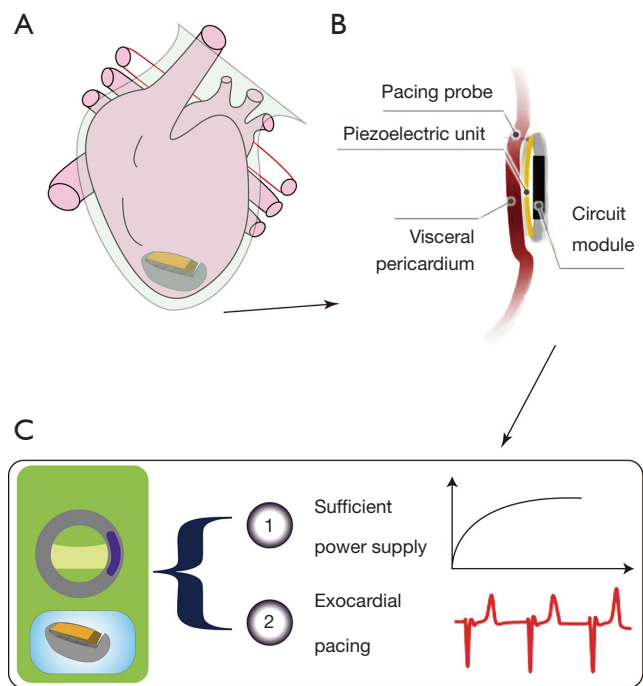


Figure 1 Concept of the self-powered pacemaker. (A) Design diagram of the self-powered cardiac pacemaker system based on piezoelectric buckling energy acquisition; (B) a partial magnification of the basic structure of the pacemaker; (C) two major challenges to the pacemaker strategy.

which is mainly composed of piezoelectric film composite structural units of flexible buckling bridge-type.

Preparation of the piezoelectric energy collector extract

The piezoelectric energy collector material was collected and sterilized by UV. The extraction medium was 10 mL DMEM culture medium containing 10% fetal bovine serum placed in an incubator at 37 °C for 24 h with 5% CO₂. After centrifugation, the supernatant was obtained, filtered, and sterilized, and stored in a 100 mL bottle at 4 °C for use within 24 h.

Cell culture

The flexible buckling piezoelectric vibratory energy collector was sterilized by UV for 15 minutes. HUVECs (from the Central Laboratory of Changhai Hospital) in the experimental group were cultured with the piezoelectric energy collector extract. The cryopreservation tube was collected from the liquid nitrogen container and directly

immersed in warm water at 37 °C. The tube was shaken to facilitate rapid thawing. The frozen storage tube was then removed from the 37 °C water bath, and the cover was opened to collect the cell suspension with a straw. The cell suspension was added into a centrifuge tube, then culture solution (10 times more) was added and well mixed. The supernatant was discarded after centrifugation at 1,000 RPM for 5 min, and the cells were resuspended in DMEM medium (Gibco, USA) with 10% fetal bovine serum (Gibco, USA) and 1% penicillin-streptomycin (Gibco, USA). After cell counting, the cell density was adjusted, and the cells were inoculated in a culture flask and incubated at 37 °C. The next day, the medium was changed to continue the culture. Then, 20 μL of cell suspension at a concentration of 1×10⁶ cells/mL was inoculated onto the surface of the sterilized flexible bending piezoelectric vibrational energy collector, and placed into a 5% CO₂ incubator and incubated at 37 °C. After 4 h, 15 mL of DMEM culture solution was added for further incubation. The culture solution was changed every 24 h. The cells of the control group were cultured in a traditional culture dish, and the medium was changed according to the abovementioned cell culture method. The whole experiment was independently repeated 3 times.

3-(4,5 dimethylthiazol-2-yl)-2,5-diphenyltetrazolium bromide (MTT) experiment

Cell viability was determined using a MTT assay. After 1, 3, and 5 days of H9C2 cell culture, samples were rinsed in phosphate buffered saline (PBS) twice. Then, 100 μL of cell suspension at 5×10³ cell/well was added into each well (the edge holes were filled with sterile PBS to eliminate the edge effect). Three wells were set in each group. A 96-well plate was used for detection every 24 hours. Then, the medium was removed, and 20 μL MTT solution (5 mg/mL) was added into each well, and the plate was cultured in a cell incubator for another 4 h. After carefully absorbing the medium in the hole using a pipette (with attention paid to the pipette head that should be close to the inner wall of the hole when absorbing the medium without touching the purple crystal at the bottom, or the 96-well plate was inverted on the filter paper to absorb the medium in the hole), 150 μL DMSO was added into each well to fully dissolve the crystals. After adding DMSO, the 96-well plates were placed into an incubator at 37 °C for 10–20 min to help the dissolution of purple crystals with DMSO. The plates were mixed for 10 min after adding DMSO. Optical

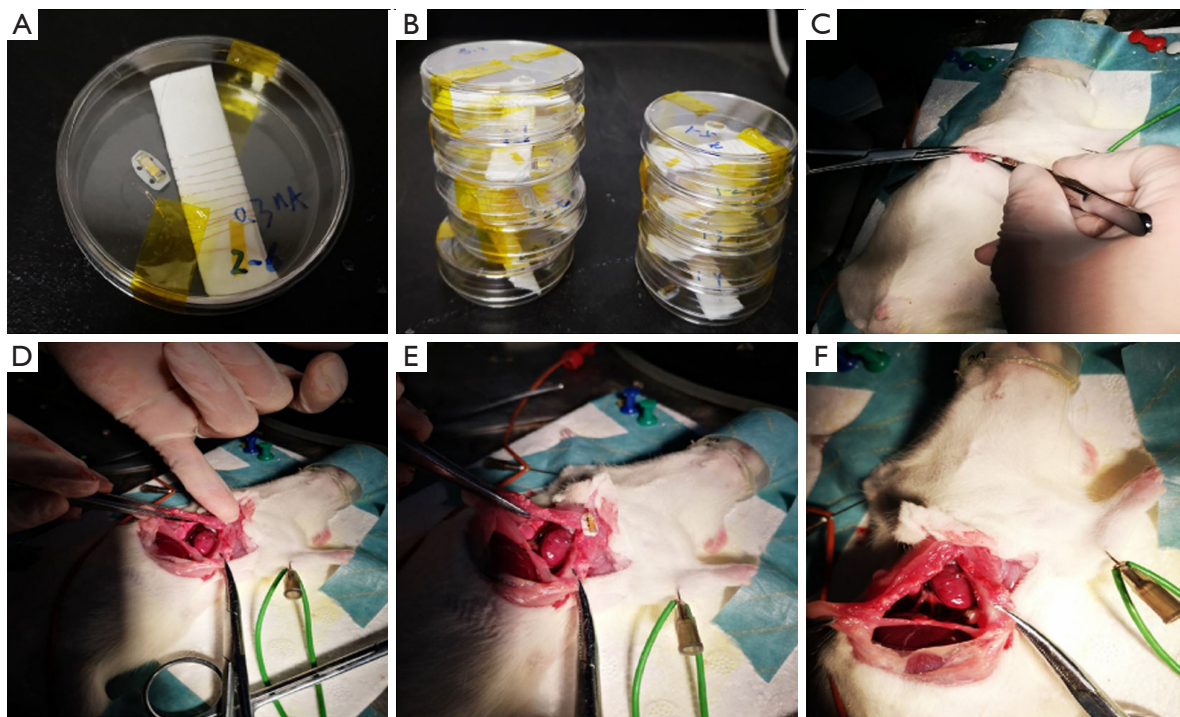


Figure 2 The process of implanting the piezoelectric vibrator near the cardiac apex. (A) The piezoelectric vibrator for rats; (B) several piezoelectric vibrators for rats; (C) chest incisions; (D) exposure of rat hearts; (E) implanted piezoelectric vibrator; (F) after implantation of the piezoelectric vibrator.

density (OD) was measured at 490 nm using a microplate meter. Cell viability (%) was calculated using the following formula: the rate of living cells = (total number of cells - number of dead cells)/total number of cells \times 100%. According to the standard ISO10993-533, cell viability above 70% was considered as non-cytotoxic.

Implant devices

Animal experiments were conducted according to the Institutional Animal Care and Use Committee (IACUC) and approved by the Naval Military Medical University (Second Military Medical University, CHEC2019-103) Animal Care Center. The *in vivo* study was conducted using SD female rats (6–7 weeks, 170–180 g) which were fasted for 12 hours before surgery. A Rodent Anesthesia Machine and isoflurane were used at a flow rate to maintain anesthesia. After anesthesia, the rats were fixed on an operating table, with the head of the table tilted 60 degrees. Hair removal cream was used to remove the chest hair and cold light was applied to the chest. Then the rats were disinfected with iodophor three times, and covered with disinfecting wipes.

The subcutaneous fascia, pectoralis major, and serratus anterior were separated by a longitudinal incision 2–3 mm from the left edge of the sternum to expose the 3rd and 4th ribs. The intercostal muscles of the 3rd and 4th ribs were obtusely separated and cut off. Then, the capsule was cut with ophthalmic scissors, and the chest was opened with eyelid openers to fully expose the bottom of the heart. Subsequently, the piezoelectric vibratory energy collector prepared with UV sterilization was quickly implanted and fixed in the pericardium facing the heart tip. The blood was removed from the chest with a cotton swab and bleeding spots were observed. After confirming that there was no bleeding, the skin was sutured with thread 0 and disinfected with iodine volt. The anesthesia machine was removed, and the rats were placed in the cages. The work flow chart is shown in *Figure 2*.

CT scanning

CT is a diagnostic technology combining computers and X-ray. Multi-slice spiral CT has been widely used in clinical practice for its high temporal resolution, high

spatial resolution, and high-density resolution. The rats were anesthetized by intraperitoneal injection of 2% sodium pentobarbital (40 mg/kg) at the 12th week after implantation of the flexible flexion piezoelectric vibratory energy absorber. Toshiba Aquilion CT imaging was performed on the chests of 10 SD rats with a thin slice of 0.5 mm. Both groups were scanned at 120 kV with a scan length of 8 cm. The rats were fixed in a supine position, and the chest was first scanned by the double positioning line, and then scanned from the thoracic inlet to the abdomen. All the images were transmitted to the Toshiba cloud workstation for post-processing and image analysis (data form: 1. BMP format: 3D local magnification, maximum density projection bone window).

Heart ultrasonography

Forty male SD rats (purchased from the Experimental Animal Center of the Second Military Medical University) were randomly divided into 3 groups, with 20 rats in the experimental group, 10 rats in the sham operation group, and 10 rats in the control group. The average weight and age of the rats were 230 g and 8 weeks old, respectively. The rats in the experimental group all received thoracotomy and piezoelectric device implantation in the thoracic cavity, those in the sham operation group only received sham thoracic surgery, and those in the control group did not receive any surgery. The ultrasonography equipment was the SequoIA 512 color Doppler ultrasound diagnostic instrument (probe frequency: 8–13 MHz), which was equipped with tissue doppler imaging, a cardiac function measurement software package, and a synchronous single-lead electrocardiogram (ECG). The weight of each group of rats was measured before anesthesia, synchronous II ECG was recorded during ultrasound examination, and heart rate was measured. The peak of the R wave was the end of diastole, and the end of the T wave was the end of systole.

After the experimental animals were weighed, 2% sodium pentobarbital (40 mg/kg) was injected into the abdominal cavity. Under anesthesia, the left chest hair was cut using a cotton ball dipped in a depilatory agent, and after 2 or 3 minutes, the rats were washed with warm water, and the depilated part was dried with gauze. The rat limbs were fixed on the operating table in supine position, and the probes were placed on their left chest. After obtaining a satisfactory short-axis two-dimensional image of the left ventricle next to the sternum at the level of the papillary muscle, M-mode echocardiograms were obtained by placing

the M-mode sampling line perpendicular to the septum and posterior wall of the left ventricle. The data were measured in 3–5 cardiac cycles to obtain the average value.

The data results were processed by SPSS V24.0 statistical software. All the data were expressed as mean \pm standard deviation. The ultrasound indexes between the three groups were analyzed by variance analysis. Among them, the homogeneity of variance index was adopted by LSD. The correlation between bivariate was analyzed by Pearson analysis.

Plasma biochemical testing

The automatic biochemical analyzer is an automatic test instrument. The biochemical operations were performed according to the kit instructions. The results of the automatic biochemical analysis and detection index were automatically generated based on the sample concentration, and the data were exported with an Excel report. In general, the absorbance was measured by a full-wavelength enzyme plate, and then the absorbance of the sample was converted into concentration according to the formula in the instruction manual.

The sample was clear and transparent, and suspended matter was removed by centrifugation (avoided using hemolyzed samples). If the samples were not tested immediately after collection, they were frozen at -80°C to avoid repeated freezing and thawing. Serum biochemical tests were performed on 10 rats (5 in the normal control group, and 5 in the experimental group implanted with a flexible buckling piezoelectric vibration energy harvester). In the ALT test program, a serum specimen in the control group (specimen No. 3) and a serum specimen in the experimental group (specimen No. 7) were hemolyzed. In statistical analysis, these two samples were removed, while the other 8 samples were used for analysis. Samples from other tests were normal. The reagent preparation and the point sample quantity were accurate, and the samples and reagents in the pipette gun were completely drained. The incubation temperature and time were accurately set strictly following the instructions.

Statistical analysis

SPSS 24.0 software was used for statistical analysis. The experimental data were expressed as mean \pm standard deviation ($\bar{x}\pm s$). The independent sample *t*-test and one-way analysis of variance (ANOVA) were applied, and the homogeneity of variance test was performed at the same

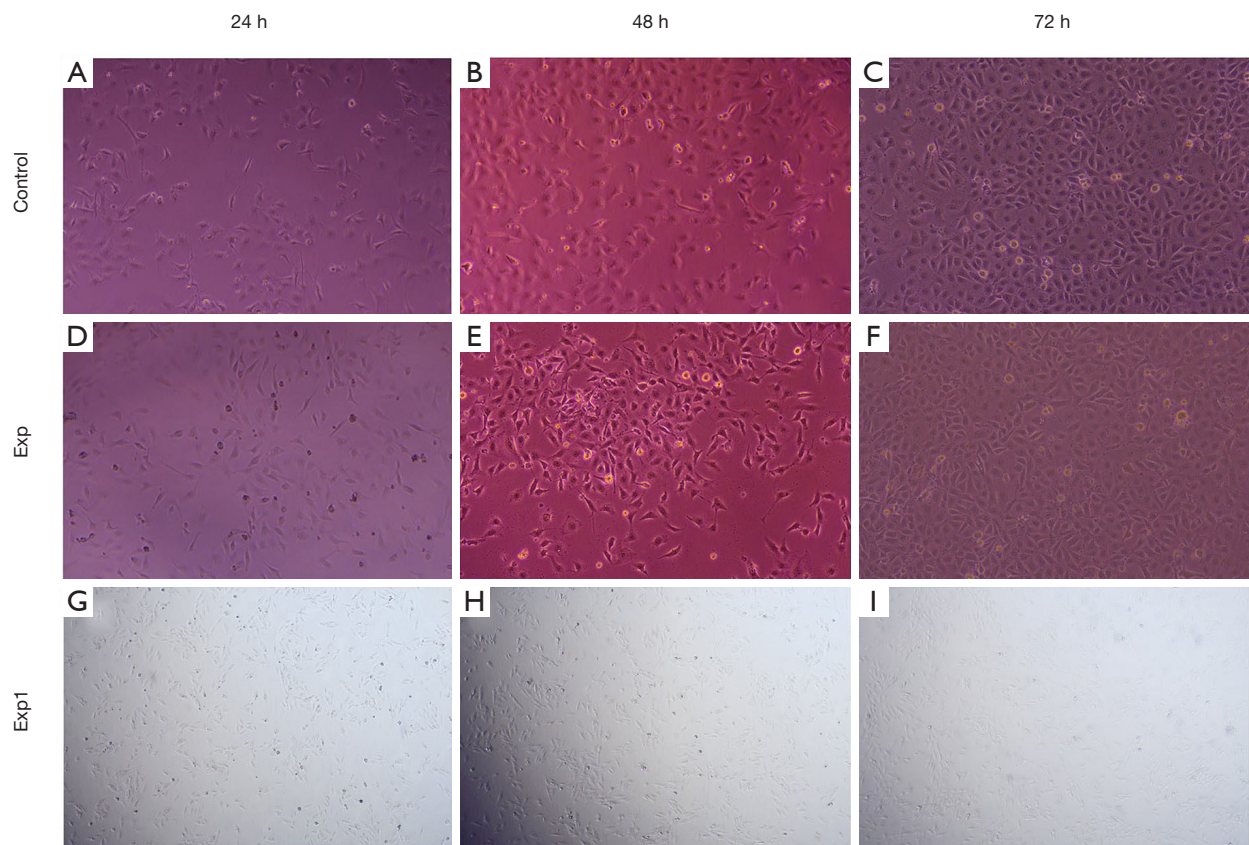


Figure 3 Impact of the piezoelectric energy harvester on cell state and morphology. Cell culture was carried out with a blank petri dish and a piezoelectric vibrational energy collector (experimental group). Both control group and experimental group 1 comprised of human HUVECs, and experimental group 2 was comprised of rat H9C2 cells. The state of cells was observed under a light microscope using a 10 \times objective lens. (A) HUVEC, 24 h; (B) HUVEC, 48 h; (C) HUVEC, 72 h; (D) HUVEC, 24 h; (E) HUVEC, 48 h; (F) HUVEC, 72 h; (G) rat H9C2 cardiomyocytes, 24 h; (H) H9C2, 48 h; (I) H9C2, 72 h.

time. When the variance was homogeneous, the LSD statistical method was used for comparisons between groups. $P < 0.05$ indicated a significant difference.

Results

Cell morphology

HUVECs adhered to the walls in the blank group and the experimental group with a cobblestone and epithelial-like appearance. After 24, 48, and 72 hours, HUVECs were in a normal condition and were growing normally (Figure 3A,B,C). Thus, we speculated that the piezoelectric vibration energy collector had no effect on cell morphology. Next, H9C2 cells were cultured in a petri dish with a sterilized piezoelectric vibration energy extractor, and it was

found that H9C2 cells normally attached to the wall and presented a long spindle shape. After 24, 48, and 72 hours (Figure 3D,E,F), the cells could still proliferate normally. Then we Culture H9C2 Rat Myocardial Cells with the same condition (Figure 3G,H,I). These results showed that the piezoelectric vibrational energy harvester had no effect on cell morphology or cell convergence. All photographs were directly obtained with an optic microscope (Axio Vert).

The results of the MTT assay in cardiomyocytes co-cultured with piezoelectric energy collector extract

The results of H9C2 cell viability and proliferation are shown in Figure 4. H9C2 cells showed a time-dependent growth pattern in all control and experimental groups. Although cells in the control group showed better

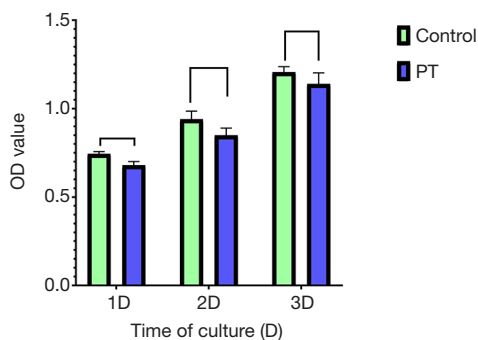


Figure 4 Cell viability was measured using a Cell Titer 96® Cell Proliferation assay after 1, 2, and 3 days of culture. PT: the experimental groups were cultured with the piezoelectric energy harvester. Control: blank control group.

proliferation than those in the experimental group after 1 and 3 days, there was no difference between the control group and the experimental group throughout the culture period ($P > 0.05$). The cell viability of the experimental group was higher than 70% during the whole culture, meaning that according to ISO10993-533, the flexible buckling piezoelectric vibrational energy collector was not cytotoxic.

CT results

Twelve weeks after the implantation of the flexible piezoelectric energy harvesting device, the A (I–III) and B (I–III) CT scan confirmed that the device was in a good position and was located between the apex of the heart and the left thoracic wall. The character “i” and “I” were the bone windows, and “ii” and “II” were the mediastinal windows. The “iii” and “III” images were reconstructed by the maximum area projection method. The results in *Figure 5* showed that the position of the flexible buckling piezoelectric vibration energy harvester did not change much at the 12th week after implantation, and it was still in the implanted position.

Cardiac ultrasound results

Comparisons of the preoperative general condition and cardiac function of each group are shown in *Table 1*, and general observations and cardiac function in each group at 12 weeks post-surgery are shown in *Table 2*. There was no significant difference among other indicators ($P > 0.05$).

According to the above results, the weights of all groups increased significantly after 12 weeks ($P < 0.05$), while heart

rate had no significant change ($P > 0.05$). Left ventricular ejection fraction (LVEF) and left ventricular fractional shortening fraction (LVFS) were not significantly decreased in the experimental group (*Figure 6*). LVEF and LVFS were increased in both the control group and sham group ($P < 0.05$). Compared with the control group and sham group, LVEF and LVFS of the experimental group were decreased after 12 weeks ($P < 0.05$).

We found that the LVEF and LVFS of rats increased with age, and that the device implanted in the thoracic cavity of rats still had certain influences on cardiac function.

Plasma biochemical test results

The results of 17 biochemical indicators showed that total bilirubin (TBIL) and triglyceride (TG) had significant differences as shown in *Table 3*. (P value, $P < 0.05$), while there was no significant difference among other indicators (*Table 3*).

Discussion

Cardiac pacemakers are common clinical implantable medical electronic therapy devices. Due to influential factors in the internal environment, pneumothorax, infection, and other adverse reactions can occur after implantation. Therefore, the biocompatibility, *in vivo* stability, and safety of implanted medical devices have become major problems to be solved for their use in the long term (16,17).

We prepared a flexible buckling piezoelectric vibrational energy collector in the early stage. In this paper, the cytotoxicity and biocompatibility of the collector as well as the stability and safety of the collector in rats were examined. In terms of the biocompatibility and cytotoxicity, HUVECs in the blank and experimental groups were in good condition, and the growth rate was normal, indicating that the piezoelectric vibration energy collector had no effect on cell morphology. Subsequently, H9C2 cells were cultured with the sterilized piezoelectric vibration energy collector in a petri dish, and the H9C2 cells could normally adhere to the wall and proliferate. These results indicated that the piezoelectric vibrational energy harvester had no effect on cell morphology and cell convergence. H9C2 cells showed a time-dependent growth pattern in all control and experimental groups. After 1 and 3 days, there was no statistical difference between the control group and the experimental group during the whole culture period ($P > 0.05$), showing that the flexible

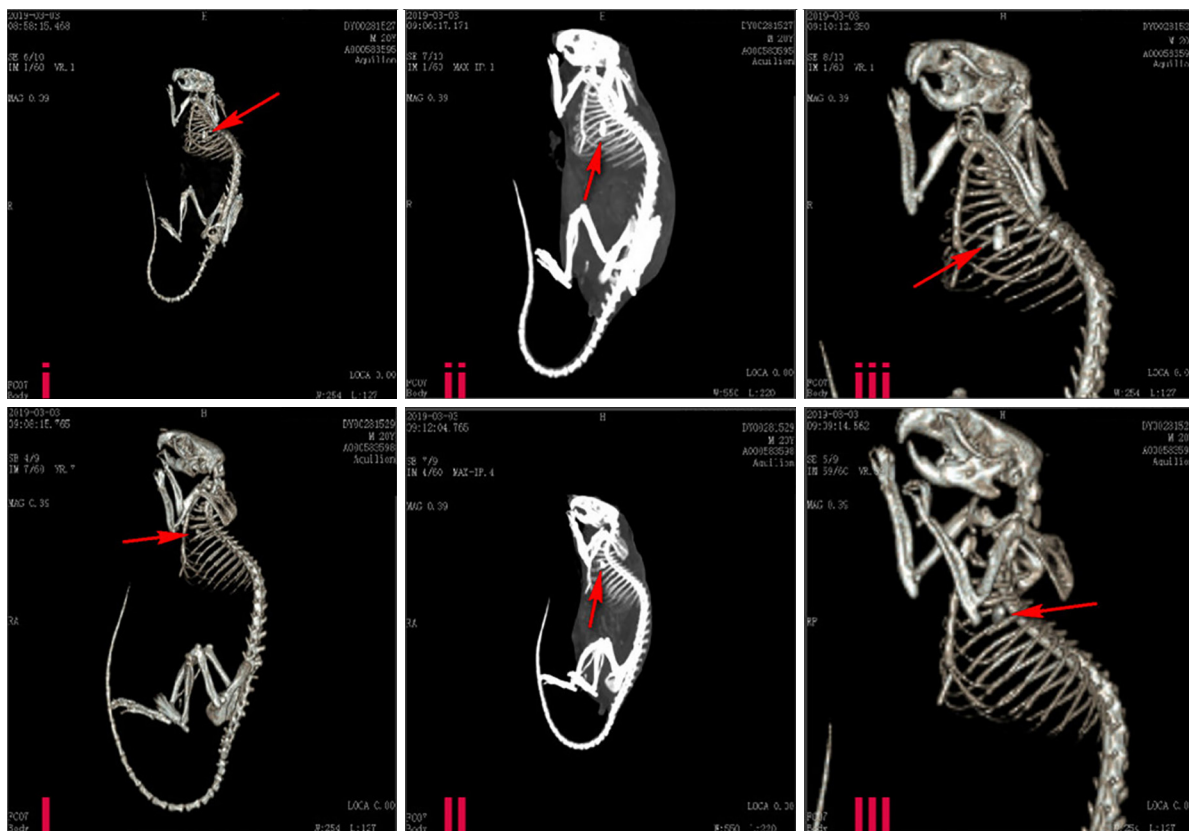


Figure 5 Position of the piezoelectric energy harvester fixed on the left ventricular surface, near the cardiac apex (representative images are shown). The red arrow indicates the position of vibration energy harvester.

Table 1 Cardiac function in each group

| Group | n | Weight (g) | Heart rate (times/min) | Ejection fraction (%) | Short axis fraction (%) |
|----------------------|----|--------------|------------------------|-----------------------|-------------------------|
| Experimental group | 20 | 230.56±12.32 | 210.60±10.23 | 82.38±10.54 | 52.68±16.43 |
| Control group | 10 | 231.02±11.97 | 208.75±11.58 | 82.19±7.50 | 52.86±10.62 |
| Sham operation group | 10 | 228.47±10.68 | 207.95±14.85 | 82.64±8.59 | 53.19±18.15 |

Table 2 General observations and cardiac function in each group at 12 weeks post-surgery

| Group | n | Weight (g) | Heart rate (times/min) | Ejection fraction (%) | Short axis fraction (%) |
|----------------------|----|--------------|------------------------|-----------------------|-------------------------|
| Experimental group | 17 | 447.68±16.12 | 209.45±12.57 | 82.03±13.24 | 51.24±8.25 |
| Control group | 10 | 450.23±9.56 | 207.50±9.76 | 86.79±11.43 | 56.31±7.47 |
| Sham operation group | 10 | 448.53±12.73 | 206.19±16.15 | 86.54±7.22 | 55.65±12.38 |

The experimental group received thoracotomy and device implantation, the control group did not receive surgical intervention, and the sham operation group only received switched thoracic surgery. The pairwise comparison of body weight, heart rate, ejection fraction, and short axis shortening fraction among groups was $P>0.05$.

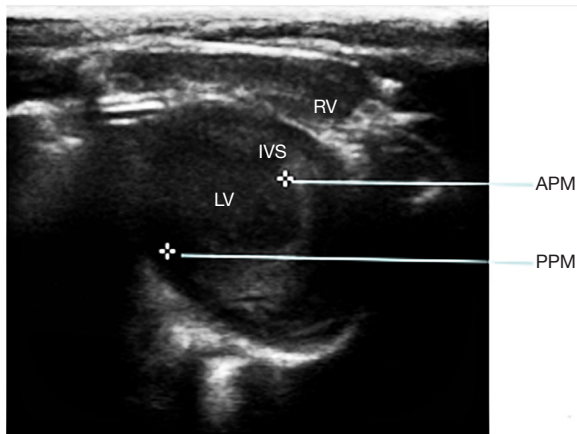


Figure 6 Horizontal view of the papillary muscle of the short axis of the parasternal left ventricle. RV, right ventricle; LV, left ventricle; IVS, interventricular septum; APM, anterior papillary muscle; PPM, posterior papillary muscle. Note: 3 rats in the experimental group died after the device was implanted.

buckling piezoelectric vibration energy harvester had no cytotoxicity. At the 12th week after implantation of the flexible flexion piezoelectric vibrational energy harvester in rats, CT showed that the position of the harvester had not changed significantly and remained in the implanted position. Ultrasonography results demonstrated that cardiac function was affected before and at 12 weeks after the implantation. The results of 17 biochemical indexes showed that there were significant differences in TBIL and TG ($P < 0.05$), but there were no significant differences in other indexes.

This paper focused on the implantable biocompatibility and *in vivo* safety of the flexible flexion piezoelectric energy absorber, and demonstrated the compatibility and safety of the absorber *in vivo* and *in vitro*. The current findings contribute to the development and clinical application of the flexible flexion piezoelectric energy collector, and has important significance for the development of new cardiac

Table 3 Comparison of the test results of 17 biochemical indexes between the control and the experimental group

| Item | Unit | Control group | Experimental group | P value |
|-------|--------|----------------|--------------------|---------|
| ALT | U/L | 78.35±31.78 | 62.86±13.7 | 0.468 |
| AST | U/L | 317.36±181.95 | 205.63±45.64 | 0.268 |
| DBIL | μmol/L | 17.93±1.52 | 11.77±1.22 | 0.051 |
| TBIL | μmol/L | 53.52±15.71 | 33.12±5.14 | 0.039* |
| ALB | g/L | 30.54±0.29 | 31.61±0.53 | 0.326 |
| ALP | U/L | 200.88±44.64 | 225.58±19.92 | 0.342 |
| r-GT | U/L | 3.27±2.62 | 2.5±1.31 | 0.612 |
| TBA | μmol/L | 27.24±5.75 | 24.74±3.96 | 0.496 |
| BUN | mg/dL | 32.54±12.69 | 25.8±2.37 | 0.327 |
| CRE | μmol/L | 56.1±6.86 | 47.72±9.73 | 0.197 |
| UA | μmol/L | 201.19±117.18 | 133.63±13.38 | 0.285 |
| CK | U/L | 435.38±1827.39 | 1,118.35±611.24 | 0.617 |
| LDH-L | U/L | 1,770.8±423.18 | 1,606.18±330.01 | 0.896 |
| TG | mmol/L | 1.55±0.35 | 1.25±0.09 | 0.02* |
| TC | mmol/L | 2.03±0.28 | 2.61±0.56 | 0.574 |
| HDL-C | mmol/L | 0.35±0.06 | 0.54±0.15 | 0.694 |
| LDL-C | mmol/L | 1.66±0.19 | 1.58±0.19 | 0.693 |

*, $P < 0.05$. If $P < 0.01$, it indicated that there was a significant difference between the 2 groups of data. If $0.01 < P < 0.05$, the 2 groups of data were significantly different. If $P > 0.05$, there was no significant difference between the 2 groups.

pacemakers.

Acknowledgments

Funding: This work was supported by the National Natural Science Foundation of China (81470592).

Footnote

Reporting Checklist: The authors have completed the ARRIVE reporting checklist. Available at <http://dx.doi.org/10.21037/atm-21-1707>

Data Sharing Statement: Available at <http://dx.doi.org/10.21037/atm-21-1707>

Conflicts of Interest: All authors have completed the ICMJE uniform disclosure form (available at <http://dx.doi.org/10.21037/atm-21-1707>). The authors have no conflicts of interest to declare.

Ethical Statement: The authors are accountable for all aspects of the work in ensuring that questions related to the accuracy or integrity of any part of the work are appropriately investigated and resolved. Animal experiments were conducted according to the Institutional Animal Care and Use Committee (IACUC) and approved by the Naval Military Medical University (Second Military Medical University, CHEC2019-103) Animal Care Center.

Open Access Statement: This is an Open Access article distributed in accordance with the Creative Commons Attribution-NonCommercial-NoDerivs 4.0 International License (CC BY-NC-ND 4.0), which permits the non-commercial replication and distribution of the article with the strict proviso that no changes or edits are made and the original work is properly cited (including links to both the formal publication through the relevant DOI and the license). See: <https://creativecommons.org/licenses/by-nc-nd/4.0/>.

References

1. Easo J, Weymann A, Hölzl P, et al. Hospital Results of a Single Center Database for Stentless Xenograft Use in a Full Root Technique in Over 970 Patients. *Sci Rep* 2019;9:4371.
2. Lissandrello CA, Santos JA, Hsi P, et al. High-throughput continuous-flow microfluidic electroporation of mRNA

- into primary human T cells for applications in cellular therapy manufacturing. *Sci Rep* 2020;10:18045.
3. Göbel CH, Göbel A, Niederberger U, et al. Occipital Nerve Stimulation in Chronic Migraine: The Relationship Between Perceived Sensory Quality, Perceived Sensory Location, and Clinical Efficacy-A Prospective, Observational, Non-Interventional Study. *Pain Ther* 2020;9:615-26.
 4. Nicolini F, Fortuna D, Contini GA, et al. Long-Term Outcomes of Conventional Aortic Valve Replacement in High-Risk Patients: Where Do We Stand? *Ann Thorac Cardiovasc Surg* 2016;22:304-11.
 5. Zhang T, Liu Y, Zou C, et al. Single chamber permanent epicardial pacing for children with congenital heart disease after surgical repair. *J Cardiothorac Surg* 2016;11:61.
 6. Machno M, Bogucki R, Szkoda M, et al. Impact of the Deionized Water on Making High Aspect Ratio Holes in the Inconel 718 Alloy with the Use of Electrical Discharge Drilling. *Materials (Basel)* 2020;13:1476.
 7. Vandeplass G, Van Heuverswyn F, Drieghe B, et al. Ultrasound-guided thoracotomy for implantation of an epicardial left ventricular lead after left pneumonectomy. *Interact Cardiovasc Thorac Surg* 2012;15:938-40.
 8. Paech C, Kostelka M, Dähnert I, et al. Performance of steroid eluting bipolar epicardial leads in pediatric and congenital heart disease patients: 15 years of single center experience. *J Cardiothorac Surg* 2014;9:84.
 9. Udink ten Cate F, Breur J, Boramanand N, et al. Endocardial and epicardial steroid lead pacing in the neonatal and paediatric age group. *Heart* 2002;88:392-6.
 10. Yang H, Pang Y, Bu T, et al. Triboelectric micromotors actuated by ultralow frequency mechanical stimuli. *Nat Commun* 2019;10:2309.
 11. Parangusan H, Ponnamma D, Al-Maadeed MAA. Stretchable Electrospun PVDF-HFP/Co-ZnO Nanofibers as Piezoelectric Nanogenerators. *Sci Rep* 2018;8:754.
 12. Lu B, Chen Y, Ou D, et al. Ultra-flexible Piezoelectric Devices Integrated with Heart to Harvest the Biomechanical Energy. *Sci Rep* 2015;5:16065.
 13. Greatbatch W. Cardiac pacemaker. US; 1979.
 14. Tong Y, Zhao X, Tan MC, et al. Cost-Effective and Highly Photoresponsive Nanophosphor-P3HT Photoconductive Nanocomposite for Near-Infrared Detection. *Sci Rep* 2015;5:16761.
 15. Yan Y, Huang LB, Zhou Y, et al. Self-aligned, full solution process polymer field-effect transistor on flexible substrates. *Sci Rep* 2015;5:15770.

16. Xeroudaki M, Thangavelu M, Lennikov A, et al. A porous collagen-based hydrogel and implantation method for corneal stromal regeneration and sustained local drug delivery. *Sci Rep* 2020;10:16936.
17. Cooke DF, Goldring AB, Yamayoshi I, et al. Fabrication of

an inexpensive, implantable cooling device for reversible brain deactivation in animals ranging from rodents to primates. *J Neurophysiol* 2012;107:3543-58.

(English Language Editor: C. Betlazar-Maseh)

Cite this article as: Xie F, Qian X, Li N, Cui D, Zhang H, Xu Z. *In vitro* and *in vivo* studies on the biocompatibility of a self-powered pacemaker with a flexible buckling piezoelectric vibration energy harvester for rats. *Ann Transl Med* 2021;9(9):800. doi: 10.21037/atm-21-1707